

Novel DNN-powered quadrupole isolation profile analysis algorithm for improved speed, measurement robustness, and quality control

Adrian Schütz, Amelia C. Peterson, Bastian Reitemeier, and Bernd Hagedorn - Thermo Fisher Scientific, Bremen, Germany

ABSTRACT

Quadrupole calibration maps a desired m/z-range of isolated ions to the voltages provided by the control electronics. One method for calibration relies on collection and analysis of isolation profiles generated by fixing the transmission range while scanning the isolation center and detecting (with another mass analyzer, e.g., of Thermo Scientific™ Orbitrap™ type) a single ion species. The analysis of an isolation profile determines parameters, such as width and center, which inform the construction of a calibration. Here, we present an isolation profile analysis algorithm¹ that reliably models isolation profiles with minimal data collection and is robust to measurement noise and profile artifacts. For production environments, the algorithm's ability to quantify and flag such artifacts provides an actionable measure for manufacturing quality control.

INTRODUCTION

In common mass spectrometry applications, the user or method (e.g. data-dependent acquisition) configures a quadrupole isolation of a specific m/z-range of ions by setting an isolation center m/z and width. These settings must be mapped to the voltages applied to the quadrupole to result in the desired isolation range. To find this mapping, many isolation profiles are recorded during calibration. Recording this data with many steps in the isolation center is time consuming (Figure 1).

Here, we present a new algorithm for analysis of isolation profiles¹, which gives precise estimates of the isolation center and width. This algorithm requires less input data and thus allows for faster calibration than the prior algorithm (Figure 2). It additionally enables the flagging of deviations from the model for quality control purposes.

MATERIALS AND METHODS

As a model, we use a piecewise function that has Gaussian-shaped edges and a constant plateau in the center (Figure 3):

$$f(x) = \begin{cases} x < c - \frac{w}{2}, h e^{-\frac{(x-x_l)^2}{2\sigma_l^2}} \\ c - \frac{w}{2} \leq x \leq c + \frac{w}{2}, h \\ x > c + \frac{w}{2}, h e^{-\frac{(x-x_r)^2}{2\sigma_r^2}} \end{cases}$$

$$x_l = c - \frac{w}{2}, x_r = c + \frac{w}{2}$$

$$\sigma_l = \frac{l}{\sqrt{2 \log(2)}}, \sigma_r = \frac{r}{\sqrt{2 \log(2)}}$$

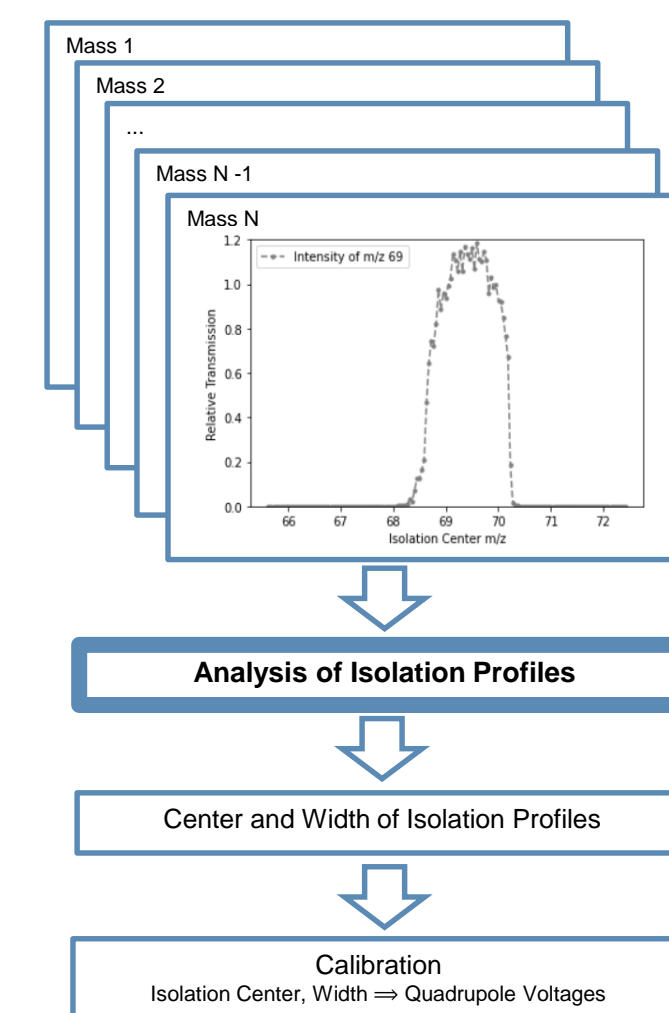
A non-linear least-squares fit (Figure 4) gives optimized model parameters for a given isolation profile. From these parameters, the center $c + \frac{r}{2} - \frac{l}{2}$ and the width $w + l + r$ can be extracted to inform the calibration.

However, the non-linear fit² can only find the global optimum if the initial parameters are already reasonably close (Figure 7). To find them, a deep neural network has been trained using the Keras library³ (Figure 5). For model training, many thousands of isolation profiles recorded during production were used. To enhance the robustness of the trained network, this data was augmented by applying shift and mirror operations as well as applying additional noise (Figure 6).

The combination of the DNN to find appropriate initial parameters and the consecutive non-linear least-squares fit shows superior performance compared to the prior algorithm (Figure 8). Even with increased step size and, in turn, less sample points during profile acquisition, it yields accurate results allowing us to reduce the calibration time.

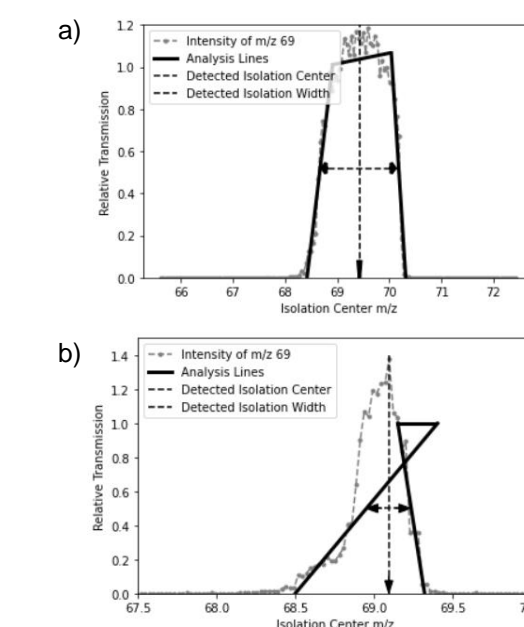
RESULTS

Figure 1. Isolation Profile Analysis for Quadrupole Calibration



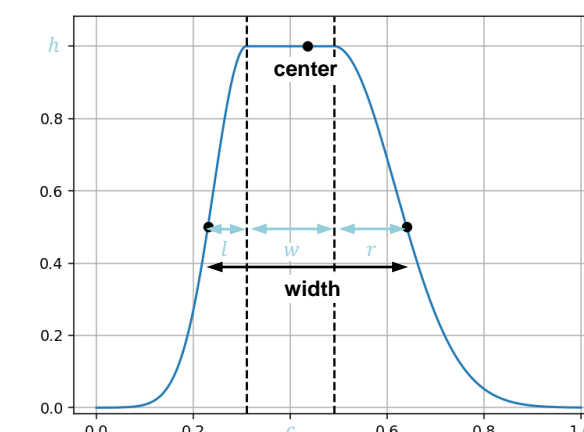
The calibration process to map from center and width of an isolation window to voltages applied to the quadrupole is carried out by recording and analyzing many isolation profiles. Here, we show an improved analysis algorithm.

Figure 2. Prior Algorithm



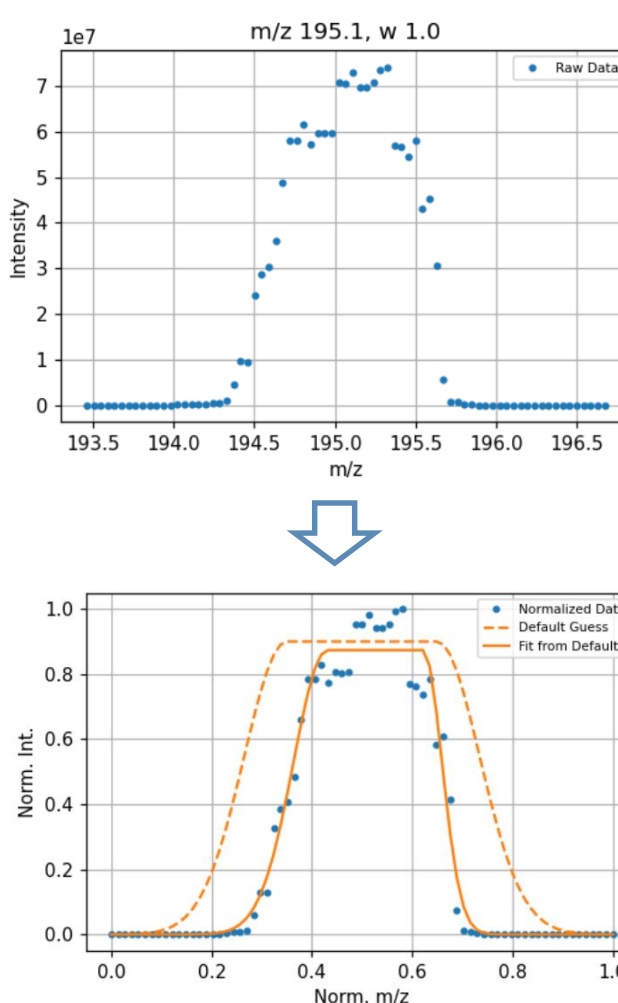
Previously, an edge-detection algorithm was used to determine the center and width of isolation profiles as shown in a). However, in rare cases the algorithm failed due to disturbances in the isolation profiles as shown in b).

Figure 3. Piecewise Model Function



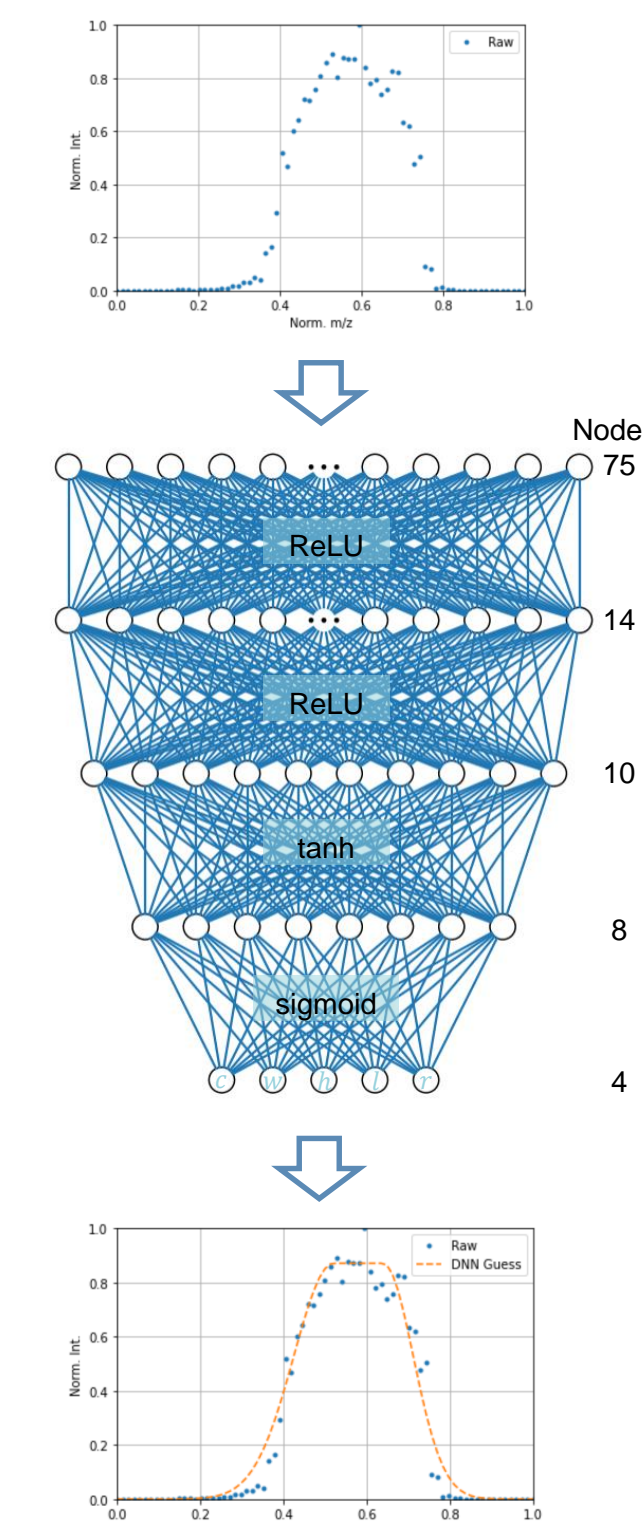
As a heuristic model, we use a piecewise function that has Gaussian-shaped edges and a constant plateau in the center. The 5 parameters of this function are the height h , the center of the plateau c , the width w of the plateau, and the half-width at half-maximum of the Gaussian edges l and r . From these parameters, we can estimate the width of the isolation profile as $w + l + r$ and the center as $c + r/2 - l/2$

Figure 4. Least-squares Fit with Default Initial Parameters



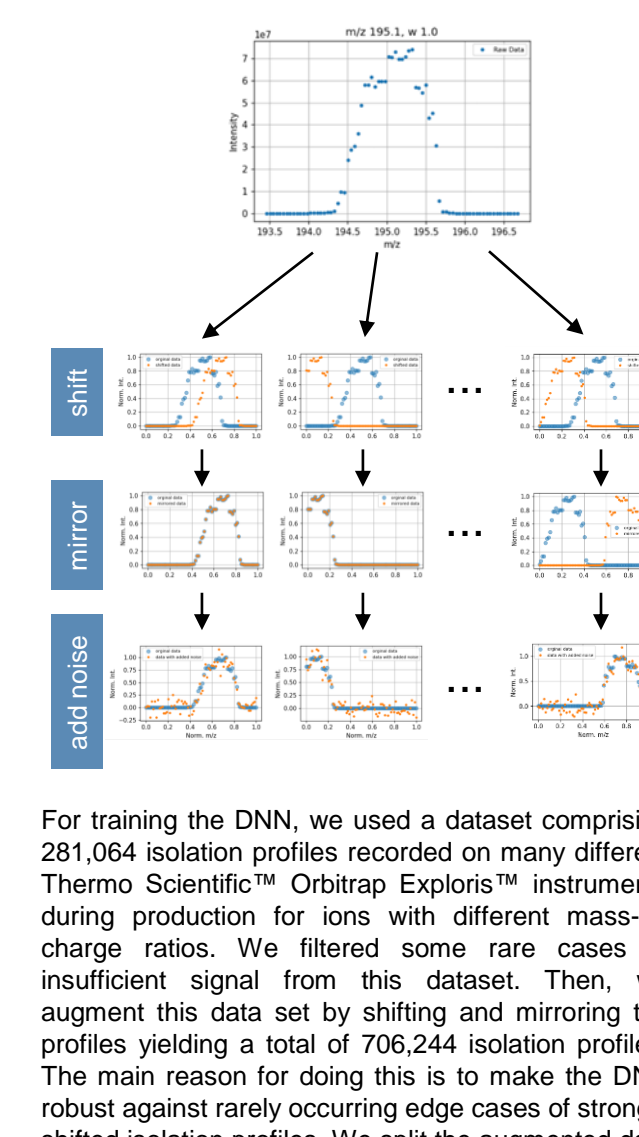
In a first approach, we normalize the isolation profile and then perform a non-linear least-squares fit² starting from default parameters. While this works in most cases, the fitting process doesn't always find the global optimum in rare cases where the default parameters are far from the global optimum. See Figure 7.

Figure 5. Deep Neural Network Architecture



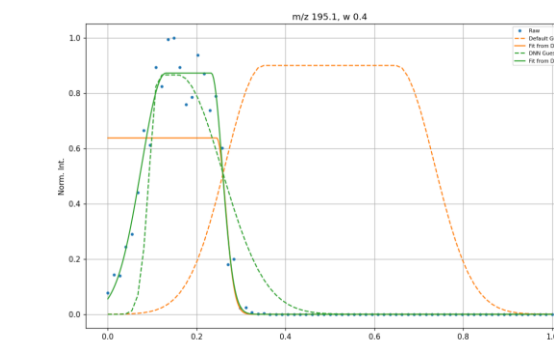
To find an initial guess for the parameters of the piecewise model function, we use a neural network which takes the normalized isolation profile as an input, passes it through a series of fully-connected layers, and finally outputs the 5 parameters for our model function. The model was trained using the Adam optimization algorithm from the Keras library³, employing the mean squared error between the fit based on the output parameters (c, w, h, l, r) and the input data as a loss function.

Figure 6. Data Augmentation



For training the DNN, we used a dataset comprising 281,064 isolation profiles recorded on many different Thermo Scientific™ Orbitrap Exploris™ instruments during production for ions with different mass-to-charge ratios. We filtered some rare cases of insufficient signal from this dataset. Then, we augment this data set by shifting and mirroring the profiles yielding a total of 706,244 isolation profiles. The main reason for doing this is to make the DNN robust against rarely occurring edge cases of strongly shifted isolation profiles. We split the augmented data set using a ratio of 75 / 25 into a training and a test set. During training, we used an additional layer adding random noise to the input data.

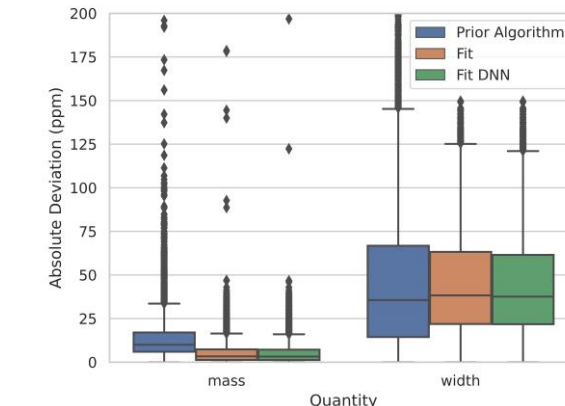
Figure 7. Corner Case to Demonstrate the Robustness of the Algorithm



For the rare case of strongly shifted isolation profiles, the default parameters are far from the global optimum. In such cases, the non-linear least-squares fit² converges to a local minimum. Using the DNN result as an initial guess improves the situation and the algorithm reliably finds the global optimum in many such corner cases.

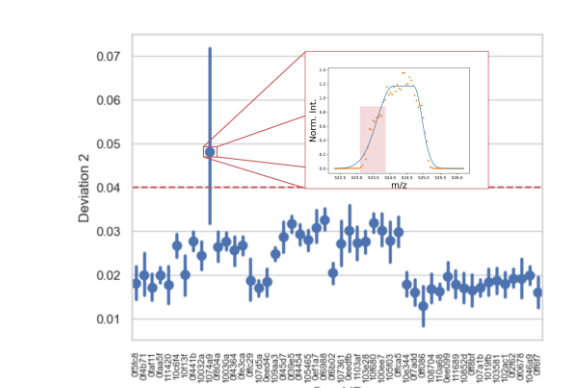
CONCLUSIONS

Figure 8. Performance Comparison



To evaluate the performance of the different algorithms, we generated a dataset of synthetic isolation profiles ($n=10,000$) with known width and center mass. Both quantities are most accurately estimated using the new algorithm.

Figure 9. Flagging Aberrant Isolation Profiles in Production



Using the residuals between fit (Deviation 2) and data on, in this case, the left flank of the profile, we can flag quadrupole of possibly poor quality. On closer inspection (inset), the isolation shapes of the quadrupole indeed display an artifact on the left edge.

In summary, the new algorithm robustly estimates the center and width of isolation profiles, which is an important prerequisite for our calibration procedure. Because the algorithm still reliably works with isolation profiles recorded with an increased step size, quadrupole calibration time can be reduced from roughly 30 minutes to about 15 minutes.

Moreover, the residuals of the fitted model function can be analyzed to flag aberrations (Figure 9). This can be an important tool for quality control and identification of hardware defects.

REFERENCES

- Adrian Schütz, Bastian Reitemeier, Amelia C. Peterson, and Bernd Hagedorn. (2021) *New Analysis Algorithm For Quadrupole Mass Filter Isolation Profiles*, European Patent Application EP21208325.7.
- Ranganathan, Ananth. (2004) *The Levenberg-Marquardt algorithm. Tutorial on LM algorithm*, 11. Jg., Nr. 1, S. 101-110.
- Gulli, Antonio; Pal, Sujit. (2017) *Deep learning with Keras*. Packt Publishing Ltd.

ACKNOWLEDGEMENTS

The authors are grateful to acknowledge the enormous contributions of fellow scientists, engineers, and other colleagues involved in the development of mass spectrometry at Thermo Fisher Scientific. A special thanks goes out to colleagues in production for recording the data and providing it to us. The authors are grateful for the support of management for the 10% project research program, which allowed us to spend 10% of our working hours on this and other related topics.

TRADEMARKS/LICENSING

© 2023 Thermo Fisher Scientific Inc. All rights reserved. All trademarks are the property of Thermo Fisher Scientific and its subsidiaries. This information is not intended to encourage use of these products in any manner that might infringe the intellectual property rights of others.

PO2023-11EN

ThermoFisher
SCIENTIFIC